Proceedings of the American Control Conference
Anchorage, AK May 8-10, 2002

Advanced Design of Disturbance Observer for High Performance Motion Control Systems

Bong Keun Kim and Wan Kyun Chung
Robotics and Bio-Mechatronics Laboratory, Pohang University of Science and Technology(POSTECH), Korea
{kbk,wkchung}@postech.ac.kr

Abstract

Disturbance observer(DOB) based controller design is one of the most popular methods in the field of motion control. In this paper, a generalized disturbance compensation framework named robust internal-loop compensator(RIC) is introduced and an advanced design method of DOB is proposed based on the RIC. Mixed sensitivity optimization problem, which is the main issue of DOB design, is also solved through the parameterization of DOB in the RIC framework. Different from conventional methods, Q-filter is separated in the mixed sensitivity optimization problem and the systematic design law for the DOB is proposed. This guarantees the robustness and optimality of the DOB and enables the design for unstable plants.

1 Introduction

Disturbance observer(DOB) based controller design is one of the most popular methods in the field of motion control. It is well known that DOB makes a system robust using Q-filter which cuts off the disturbance in low frequency region. From the DOB structure of Fig. 1, the output y can be expressed as follows:

$$y = \left[P_n(s)u_r + P_n(s)\{1-Q(s)\}d_{ex} - Q(s)\xi\right]\frac{P(s)}{\mathcal{X}(s)}, \quad (1)$$

where $\mathcal{X}(s) = P_n(s) + [P(s) - P_n(s)]Q(s)$, u_r is the reference control input, d_{ex} is the external disturbance, and ξ is the measurement noise. Below the cutoff frequency of $Q(s)$, $|Q(j\omega)| \approx 1$ is achieved. Hence the behavior of real plant $P(s)$ is to be the same as given nominal model $P_n(s)$. On the other hand, above the cutoff frequency of $Q(s)$, $|Q(j\omega)| \approx 0$ is achieved. Hence high frequency measurement noise is attenuated. Therefore, the most important parameter of the DOB design is the low-pass filter Q, and the main concern is the tradeoff between making $|Q(j\omega)|$ small and $|1-Q(j\omega)|$ small. Ohnishi used a first order filter for Q [1]. Umeno and Hori refined the DOB based on the 2-DOF controller and suggested Q-filter which has the form of

$$Q(s) = \left[1 + \sum_{k=1}^{N-r} a_k(\tau s)^k\right]\left[1 + \sum_{k=1}^{N} a_k(\tau s)^k\right]^{-1} \quad (2)$$

where N is the order of $Q(s)$, τ is a filter time constant, and r is the relative degree of $Q(s)$ [2]. Yamada *et al.* proposed a high order DOB which can achieve rapid response and lower sensitivity to the disturbance by virtue of higher order integral element [3]. But, they also showed that the high order DOB causes less damping characteristics because of large phase lag. Recently, a generalized disturbance compensating framework based on the Lyapunov

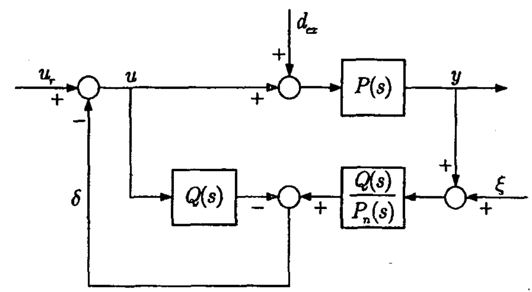

Figure 1: Disturbance observer

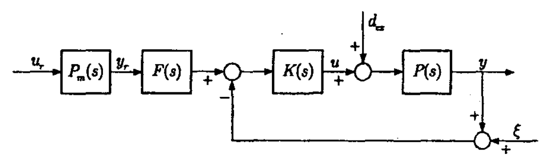

Figure 2: Compensated unity feedback system with prefilter

redesign, named robust internal-loop compensator(RIC), was proposed to show the inherent structural equivalence of the robust control algorithms [4], and unified analysis and design were performed [5]. In this paper, RIC is introduced and an advanced design method of DOB is proposed based on the RIC. Mixed sensitivity optimization problem, which is the main issue of DOB design, is also solved through the parameterization of DOB. By virtue of this, Q-filter is separated in the mixed sensitivity optimization problem and the systematic design law for the DOB is proposed. This guarantees the robustness and optimality of the DOB and also enables the design for unstable plants.

2 Robust Internal-Loop Compensator

2.1 Compensated Feedback System

Figure 2 shows a compensated feedback system with prefilter $F(s)$ to make $P(s)$ with d_{ex} behave like a given reference model $P_m(s)$. y_r is a reference model output, u is a control input, $K(s)$ is a feedback compensator. From Fig. 2, the sensitivity and complementary sensitivity functions are obtained as follows:

$$S(s) = \frac{y}{P(s)\,d_{ex}} = \frac{1}{1+L(s)}, \quad T(s) = -\frac{y}{\xi} = \frac{L(s)}{1+L(s)} \quad (3)$$

where $L(s) = P(s)K(s)$. Hence it can be easily seen that the effect of d_{ex} and ξ on y are only determined by $P(s)$ and $K(s)$.

0-7803-7298-0/02/$17.00 © 2002 AACC

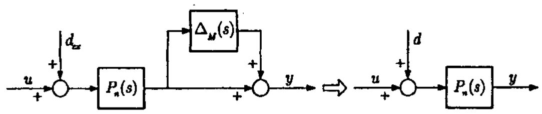

Figure 3: Reconstruction of plant

That is, $P_m(s)$ and $F(s)$ do not have an effect on $S(s)$ and $T(s)$ of Fig. 2. The transfer function from y_r to y is given by

$$T_{y_r y}(s) = F(s)\left[\frac{L(s)}{1+L(s)}\right]. \tag{4}$$

Thus, $F(s)$ is just used to make $T_{y_r y}(s) = 1$. Therefore, the design objective is to design $K(s)$ and $F(s)$ so that the specified robustness and performance are achieved under the parametric uncertainty and disturbance condition.

2.2 Prefilter Design

In order to design $F(s)$, we need to reconstruct the given system to the system which has $P_n(s)$ and redefined disturbance d. Let the plant with uncertainty be expressed as $P(s) = P_n(s)\left[1+\Delta_M(s)\right]$ where $\Delta_M(s)$ is an allowable multiplicative uncertainty. Then, the plant can be reconstructed as shown in Fig. 3. From this figure, d is expressed as

$$d = \Delta_M(s)\,u + \left[1+\Delta_M(s)\right] d_{ex}, \tag{5}$$

which satisfies an important structural property called as *matching condition*. Thus, if $F(s)$ is designed as

$$F(s) = \left[\frac{L_n(s)}{1+L_n(s)}\right]^{-1} = \frac{1}{G_{L_n}(s)} \tag{6}$$

where $L_n(s) = P_n(s)K(s)$, then $|T_{y_r y}(j\omega)| \approx 1$ can be achieved. However, unstable pole-zero cancellation can be occurred in (4). That is, if $P(s)$ has unstable poles in RHP, the $P_n(s)$ also has the unstable poles because $\Delta_M(s) = \left[P(s) - P_n(s)\right]/P_n(s)$. Therefore, it is not desirable that $F(s)$ is designed as $G_{L_n}^{-1}(s)$ although $G_{L_n}(s)$ is stable. Based on Fig. 2, one of the best candidates for $F(s)$ can be chosen as follows:

$$F(s) = \left[\frac{L_m(s)}{1+L_m(s)}\right]^{-1} = \frac{1}{G_{L_m}(s)} \tag{7}$$

where $L_m(s) = P_m(s)K(s)$. Thus $|T_{y_r y}(j\omega)| \approx 1$ can be achieved. Prefilter $F(s)$, in a crude way, approximates PD type control. Therefore this enhances transient performance and leads the phase of the unity feedback system in Fig. 2.

Alternatively, Fig. 2 with (7) can be equivalently transformed into Fig. 4 [5, 6]. In this figure, model following error is defined as $e_r = y_r - (y + \xi)$. Then, the control input has the form of

$$u = u_r + K(s)\,e_r + u^*, \tag{8}$$

where u^* is an optional control input to compensate nonlinear disturbances [7]. Note that the second term on the right-hand side in (8) can be interpreted as a control input based on Lyapunov redesign [4]. In this paper, the structure in Fig. 4 with the control input (8) is defined as robust internal-loop compensator(RIC) [8]. From Fig. 4, y can be expressed in terms of u_r, d_{ex}, and ξ:

$$y = \left[\{1+L_m(s)\}\,u_r + d_{ex} - K(s)\xi\right]\frac{P(s)}{1+L(s)}. \tag{9}$$

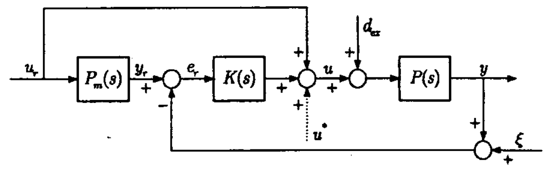

Figure 4: Robust internal-loop compensator

As a result, $S(s)$ and $T(s)$ are obtained as before. Therefore, if $K(s)$ is designed in optimal sense, the specified robustness and performance can be achieved. And also this makes the $P(s)$ behave like $P_m(s)$.

3 DOB in the RIC Framework

3.1 Analysis and Design of DOB

In this paper, unlike the typical design method of Q-filter for DOB, we propose a systematic design method in the proposed RIC framework. First, let us analyze DOB in the RIC framework. To do this, $P_m(s)$ and $F(s)$ of RIC are chosen as follows:

$$P_m(s) = P_n(s), \quad F(s) = \left[\frac{L_n(s)}{1+L_n(s)}\right]^{-1} = \frac{1}{Q(s)}, \tag{10}$$

where $P_n(s)$ is a proper function without RHP poles. Thus, $Q(s)$ is given by the nominal closed-loop system. After recalculating this equation for $K(s)$, if $K(s)$ is substituted into Fig. 4, then DOB in Fig. 1 is obtained. This means that if $K(s)$ is designed for $P_n(s)$ in order to satisfy a given criterion, optimal Q-filter is systematically designed which has the optimality under the given specific conditions, because the the feedback system with $P_n(s)$ and $K(s)$ is $Q(s)$. The disturbance attenuation characteristics of the designed system can be easily analyzed based on $Q(s)$ and also the estimated disturbance δ of DOB can be reformulated($u^* = 0$):

$$\delta = -K(s)\,e_r. \tag{11}$$

Consider a high-speed/high-accuracy positioning systems as one of the specific applications. Thus, $P_n(s)$ can be chosen as a 2nd order system and if $K(s)$ is designed as a PD controller:

$$P_n(s) = \frac{1}{J_n s^2 + B_n s}, \qquad K(s) = K_p + K_d s \tag{12}$$

where $K_p = gB_n$ and $K_d = gJ_n$, then the following Q-filter of DOB is obtained from (10):

$$Q(s) = \frac{g}{s+g}, \tag{13}$$

which is the first order filter [1]. It is notable that if $P_n(s)$ is chosen as a double integrator plant($B_n = 0$), then a derivative controller can be obtained to achieve the same $Q(s)$ in (13). More specially, consider the case that the given task is to achieve about ϕ rad phase lead effect at specified frequency with PI controller. Thus, $K(s)$ should be designed as a lead compensator with PI controller:

$$K(s) = K_L\left(\frac{Ts+1}{\alpha Ts+1}\right)\left(1+\frac{1}{T_I s}\right), \tag{14}$$

where $T_I = J_n/B_n$ and $\alpha = \frac{1-\sin(\phi)}{1+\sin(\phi)}$. From (10), therefore $Q(s)$ has the form of

$$Q(s) = \frac{Ts+1}{\left(\frac{J_n\alpha T}{K_L}\right)s^3 + \left(\frac{J_n}{K_L}\right)s^2 + Ts + 1} \tag{15}$$

and the frequency where the phase is maximum is given by $\omega_{\max} = \frac{1}{T\sqrt{\alpha}}$. If $K_L = J_n/(3\tau^2)$, $T = 3\tau$, and $\alpha = 1/9$ are substituted into (15), then $Q(s)$ is expressed as

$$Q(s) = \frac{3(\tau s)+1}{(\tau s)^3+3(\tau s)^2+3(\tau s)+1}, \qquad (16)$$

which is well known Q_{31}-filter [9]. This analysis gives very important meaning to the design of Q-filter. It is notable to see that the maximum phase contribution of the lead compensator in (14) and the frequency where the phase is maximum are obtained as

$$\phi_{\max} = \sin^{-1}\left(\frac{1-\alpha}{1+\alpha}\right) = 53^\circ, \qquad \omega_{\max} = \frac{1}{\tau}. \qquad (17)$$

The PI controller part in (14) reduces the steady state error at the cost of a phase decrease below $\omega = B_n/J_n$. Therefore, B_n/J_n should be located at a frequency substantially less than the crossover frequency so that the system's phase margin is not affected very much. This quantitative analysis and design was difficult in the previous typical DOB design. This implies that the proposed unified framework can provide a systematic insight in the design of $Q(s)$. Instead of selecting $Q(s)$, we can design $Q(s)$ from $P_n(s)$ and $K(s)$ which can produce desired specification. This is the basic difference in the design of $Q(s)$ from other previous methods. Note also that these analyses were obtained for the unity feedback system in Fig. 2. By using (10), it can be shown that the structure of DOB is also equivalently changed to the structure of RIC in Fig. 2 with $P_n(s)$. Thus, $F(s)$ in (10) is approximated to PD type controller if we use (13) or (15) and this leads the phase of the closed-loop system. Therefore, in order to design DOB with optimal sense, the characteristics of the unity feedback system and $F(s)$ should be considered at the same time.

3.2 Simulation

3.2.1 Comparative Simulation: The RIC and DOB are simulated in MATLAB environment. Let the real plant with uncertainty be expressed as

$$P(s) = \frac{1}{Js^2+Bs} = \frac{1}{(J_n+\Delta_J)s^2+(B_n+\Delta_B)s} \qquad (18)$$

where $J_n = 0.3$ V/(m/s^2) and $B_n = 0.15$ V/(m/s) are the nominal value of J and B, and Δ_J and Δ_B are their estimation errors. Thus, the nominal model $P_n(s)$ is given by $\frac{1}{J_n s^2+B_n s}$ and the multiplicative uncertainty can be obtained as $\Delta_M(s) = -\frac{\Delta_J s+\Delta_B}{(J_n+\Delta_J)s+(B_n+\Delta_B)}$. If the parameter uncertainties are given by $\Delta_J = -0.1$ V/(m/s^2) and $\Delta_B = -0.05$ V/(m/s), then $|\Delta_M(j\omega)|$ is 0.5 for all ω. Stiction and Coulomb friction are also added to the plant, whose magnitudes are 0.2 V and 0.1 V respectively. Fig. 5 shows the overall control structure. The feedback controller $C(s)$ is chosen as PD controller:

$$C(s) = K_p + K_d s \qquad (19)$$

where $K_p = 5000$ and $K_d = 300$. The feedback signal is measured through the sensor that has 2 μm resolution. The velocity is estimated by the backward differentiation of position signal. The 5th order polynomial function is used as desired trajectory:

$$y_d = y_t\left[6\left(\frac{t}{T_r}\right)^5 - 15\left(\frac{t}{T_r}\right)^4 + 10\left(\frac{t}{T_r}\right)^3\right] \qquad (20)$$

where y_t is the target position given by 30 mm and T_r is the rising time given by 0.5 s. Control sampling frequency is 1000 Hz and

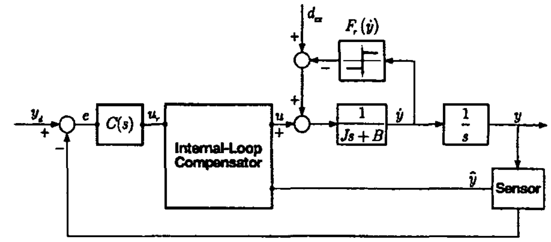

Figure 5: Overall control system and internal-loop compensators

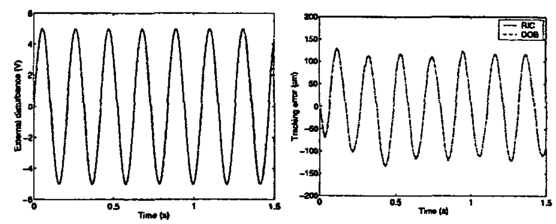

(a) External disturbance (b) Tracking error

Figure 6: Simulation results of RIC and DOB

all controllers are discretized by using the bilinear transformation. $P_m(s)$ is chosen as the same as $P_n(s)$ and $K(s)$ is chosen as PD control in (12) where g is 100. By using (10), the $Q(s)$ of DOB used in Fig.5 is calculated as $\frac{g}{s+g}$, which provides same control environment. To compare and verify the simulation results, the disturbance shown in Fig. 6 (a) is added to control input, where the signal is a 30 rad/s sinusoid. Fig. 6 (b) shows tracking errors when the two internal-loop compensators are applied to the system of Fig. 5. As can be seen here, the results show the equivalent characteristics of RIC and DOB. Of course, the other parameters such as more optimized $Q(s)$ of DOB can be selected to further improvement of performance and disturbance attenuation. But the point is that it can be always shown that there is an equivalence between them through RIC framework such as (10).

3.2.2 $Q(s)$ Design: In order to show that the proposed RIC structure gives a general design framework for the DOB algorithm, a simple design example is shown in this section. Now, let the task be to achieve about 30° phase lead effect at specified frequency with PI controller in the DOB closed-loop. Thus, the lead compensator in (14) should be used. From this, α is obtained as 1/3 and if $K_L = J_n/(3\tau^2)$ and $T = 3\tau$, then $Q(s)$ is obtained by

$$Q(s) = \frac{3(\tau s)+1}{3(\tau s)^3+3(\tau s)^2+3(\tau s)+1} \qquad (21)$$

and $\omega_{\max} = \frac{1}{\sqrt{3}\tau}$. If $\omega_{\max}$ is set to 65 rad/s, then bode magnitude plots of $Q(s)$, $1-Q(s)$, and the tracking error when the DOB with this $Q(s)$ is applied to the system of Fig. 5 are obtained as shown in Fig. 7. The results for $Q_{31}(s)$ of (16) which has the same cutoff frequency as $Q(s)$ in (21) are also shown in this figure. It is notable that the characteristics of $1-Q(s)$ and $1-Q_{31}(s)$ are nearly the same in the low frequency range. In Fig. 7 (c), the tracking error of the newly designed $Q(s)$ shows better performance than that of $Q_{31}(s)$. Through these results, it can be easily seen that Q-filter of DOB can be systematically designed based on $P_m(s)$ and the designed $K(s)$ in the RIC framework. And also, many kinds of control methods based on feedback error such as LQ, $\mathcal{H}_2$, and

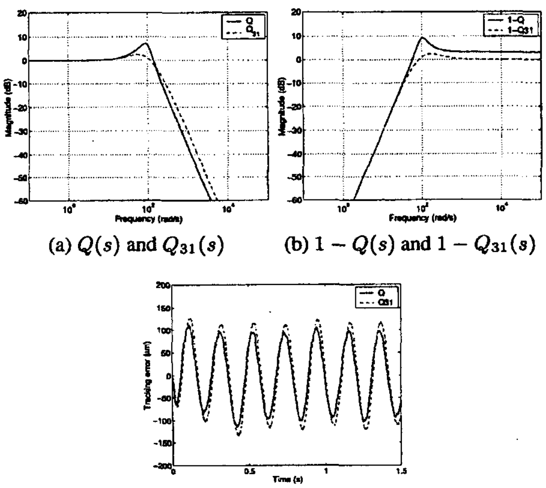

(a) $Q(s)$ and $Q_{31}(s)$ (b) $1-Q(s)$ and $1-Q_{31}(s)$

(c) Tracking error

Figure 7: Designed $Q(s)$, $Q_{31}(s)$ and tracking error

$\mathcal{H}_\infty$ control can be used to design $K(s)$ and $Q(s)$ for perturbed $P_n(s)$ in a similar manner. On the other hand, the typical DOB design framework did not present any design method for $Q(s)$ itself which can meet the above task.

4 Optimal Design of DOB

In this section, a mixed sensitivity optimization problem, which is the main issue of DOB design, is dealt with based on the structural equivalence between DOB and RIC. This gives the systematic design law for the DOB design and also guarantees the robustness and optimality of the DOB.

4.1 Mixed Sensitivity Optimization

From (1), the $S(s)$ and $T(s)$ of DOB are obtained as follows:

$$S_{DOB}(s) = \frac{P_n(s)\,[1-Q(s)]}{\mathcal{X}(s)}, \quad T_{DOB}(s) = \frac{P(s)Q(s)}{\mathcal{X}(s)}. \quad (22)$$

In this equation, if $P(s)$ can be described as $P_n(s)\,[1+\Delta_M(s)]$ and the disturbance can be formulated as (5), then the following equations can be achieved:

$$S_{DOB}(s) \approx 1-Q(s), \qquad T_{DOB}(s) \approx Q(s). \quad (23)$$

In this case, the mixed optimization problem of the $S_{DOB}(s)$ and $T_{DOB}(s)$ in (22) is changed to the $1-Q(s)$ and $Q(s)$ optimization problem. Thus, as discuss before, the most important design parameter of the DOB design becomes $Q(s)$. Therefore the trade-off between making $|\,Q(j\omega)\,|$ small and $|\,1-Q(j\omega)\,|$ small is the main issue in the DOB design. In order to meet this condition, the following optimization method has been widely used [2]:

$$\min_{a_k}\sup_{\omega}\,\left[\,|\,W_1(j\omega)\,\{1-Q(j\omega)\}\,|^2 + |\,W_2(j\omega)Q(j\omega)\,|^2\,\right] \quad (24)$$

where a_k is the parameters of (2) and $W_1^{-1}(s)$, $W_2^{-1}(s)$ are given by the ideal $S(s)$ and $T(s)$, respectively. One of the typical solutions for (24) is to choose $Q(s)$ such that the right hand side slop of $|\,Q(j\omega)\,|$ is the same as the left hand side slope of $|\,1-Q(j\omega)\,|$. With (2) and (23), $S_{DOB}(s)$ and $T_{DOB}(s)$ are obtained as

$$S_{DOB}(s) \approx \left[\frac{\tau^{N-r+1}\sum_{k=0}^{r-1} a_{N-r+1+k}(\tau s)^k}{1+\sum_{k=1}^{N} a_k(\tau s)^k}\right] s^{N-r+1},$$
$$T_{DOB}(s) \approx \frac{1+\sum_{k=1}^{N-r} a_k(\tau s)^k}{1+\sum_{k=1}^{N} a_k(\tau s)^k}. \quad (25)$$

In the frequency domain, the slope of $|\,1-Q(j\omega)\,|$ in low frequency and the slope of $|\,Q(j\omega)\,|$ in high frequency are respectively approximated as

$$\frac{Lm\,|\,1-Q(j\omega)\,|}{Lm(\omega)} \approx N-r+1, \quad \frac{Lm\,|\,Q(j\omega)\,|}{Lm(\omega)} \approx -r, \quad (26)$$

where Lm is log magnitude. Since the optimal $Q(s)$ is obtained by letting the slope be equivalent, the following relation is achieved:

$$r = \frac{N+1}{2}. \quad (27)$$

Therefore, if r is increased by n, the N is increased $(2n-1)$, where r should be designed such that it is equal to or greater than the relative degree of $P_n(s)$. Here, it is notable that the first order filter is obtained as the minimum order Q-filter for first order system [1] and the Q_{31}-filter is obtained as that for second order system [9] in the slope equivalence optimization problem of (26). On the other hand, if the disturbance can not be defined such as (5) or a specified target transfer function is given for the DOB design, it can not be said that the optimization of $Q(s)$ based on (23) is the sensitivity optimization of DOB. From (22), the real $S_{DOB}(s)$ and $T_{DOB}(s)$ are obtained as follows:

$$S_{DOB}(s) = \frac{1-Q(s)}{1+\Delta_M(s)Q(s)}, \quad T_{DOB}(s) = \frac{[1+\Delta_M(s)]Q(s)}{1+\Delta_M(s)Q(s)}. \quad (28)$$

Thus, if $|\,\Delta_M(j\omega)\,|$ is increased, (23) can not be satisfied. Although the disturbance is formulated as (5), it can be easily seen that the approximated sensitivity optimization using (23) is not an exact optimization because the magnitude of the disturbance is highly amplified. As a matter of fact, there are many cases that disturbance (5) can not be achieved [10] and the target model should be specified [11, 12]. Moreover, if $P(s)$ is unstable, $P_n(s)$ is also chosen to be unstable in conventional DOB. Thus conventional design method does not give any solution to this problem.

Now, let us consider the case that the given task of DOB is to achieve a specified transfer function of $P_m(s)$. By substituting $P_m(s)$ into $P_n(s)$ in (22), the equations are rewritten as follows:

$$S_{DOB}(s) = \frac{P_m(s)\,[1-Q(s)]}{\mathcal{X}_m(s)}, \quad T_{DOB}(s) = \frac{P(s)Q(s)}{\mathcal{X}_m(s)}. \quad (29)$$

where $\mathcal{X}_m(s) = P_m(s) + [P(s) - P_m(s)]Q(s)$. Since $P_m(s)$ can be given as an arbitrary strictly proper transfer function without RHP poles, the difference between $P(s)$ and $P_m(s)$ can be amplified. Thus, from (28), it can be seen that the optimization $Q(s)$ itself based on (23) has no meaning related to the mixed sensitivity optimization of the DOB. To cope with this problem, the DOB design should be considered in the proposed RIC framework. If the prefilter $F(s)$ of RIC is chosen as the inverse of $Q(s)$:

$$F(s) = \frac{1}{Q(s)} = \left[\frac{L_m(s)}{1+L_m(s)}\right]^{-1}, \quad (30)$$

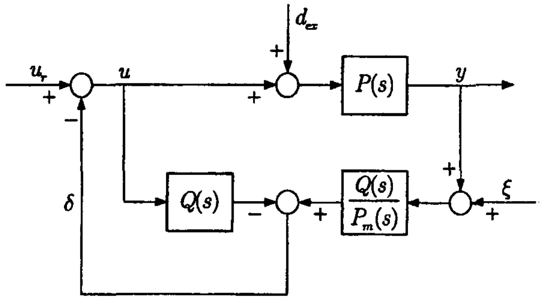

Figure 8: Disturbance observer with a reference model $P_m(s)$.

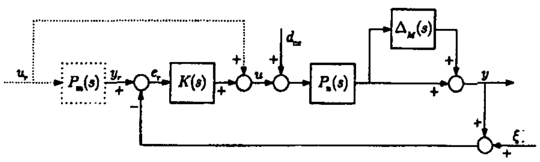

Figure 9: Mixed sensitivity optimization using $K(s)$

then similarly as shown in the previous section, the structure of RIC is equivalently changed to the structure of DOB with $P_m(s)$ instead of $P_n(s)$. Fig. 8 shows the DOB with $P_m(s)$. Thus, the optimization problem of $S(s)$ and $T(s)$ in (9) is exactly the same as the mixed sensitivity optimization problem of DOB with $P_m(s)$. From (9), $S_{DOB}(s)$ and $T_{DOB}(s)$ are given by

$$S_{DOB}(s) = \frac{1}{1+L(s)}, \qquad T_{DOB}(s) = \frac{L(s)}{1+L(s)}, \qquad (31)$$

which can also be obtained by substituting (30) into (29). In (29), $S_{DOB}(s)$ and $T_{DOB}(s)$ are the functions of $Q(s)$. But in (31), $S_{DOB}(s)$ and $T_{DOB}(s)$ are not the functions of $Q(s)$. Note here that these are the typical sensitivity and complementary sensitivity optimization problem with $P(s)$ and $K(s)$. This means that even though we introduced $P_m(s)$, the selection of $P_m(s)$ is independent of the resulting optimization problem of (31). Fig. 9 shows the control system for the mixed sensitivity optimization using $K(s)$. Therefore, variety of control methods based on feedback error can be used to design optimal compensator $K(s)$ for $P(s)$(perturbed $P_n(s)$), such as LQ, $\mathcal{H}_2$, and $\mathcal{H}_\infty$ control. This is really a simple problem. After designing optimal $K(s)$ for $P_n(s)$ with perturbations, Q-filter of DOB can be later obtained by using (30) for the reference model $P_m(s)$. Even when $P_n(s)$ is an unstable system with RHP poles, the stability of DOB is always guaranteed only if $K(s)$ is designed so that the unity feedback system with $P_n(s)$ and $K(s)$ is stable. Therefore, different from the conventional design method of (24), Q-filter design is completely separated in the mixed sensitivity optimization problems of DOB although it has implicit relation with Q-filter. And also, although the Q-filter is separately designed with sensitivity function, the proposed DOB with $P_m(s)$ has the exactly same characteristic as before. This is verified in the following.

4.2 Robust Stability Analysis

It can be said that the second issue of the DOB design is the robust stability related to the selection of a reference model $P_m(s)$. From the block diagram in Fig. 8, the input-output relationship of the DOB with $P_m(s)$ is expressed as

$$y = \left[P_m(s)u_r + P_m(s)\{1-Q(s)\}d_{ex} - Q(s)\xi\right]\frac{P(s)}{\mathcal{X}_m(s)}. \quad (32)$$

In the above equation, it can be easily seen that the DOB with $P_m(s)$ has the exactly same characteristics as before although Q-filter is separately designed with the sensitivity function of the DOB. From (32), the robust stability condition of the generalized DOB can be stated in the following theorem.

Theorem 1 *Let the plant be modeled as* $P(s) = P_n(s)[1+\Delta_M(s)]$ *with allowable multiplicative uncertainty. If the model* $P_n(s)$ *is a minimum phase system,* $P_m(s)$ *is a minimum phase system without RHP poles, and linear compensator* $K(s)$ *can stabilize* $P_n(s)$*, then a sufficient condition for robust stability of the closed-loop system of Fig. 8 for* $\Delta_M(s)$ *is given by*

$$|\Delta_M(j\omega)| < \frac{1}{|T^n_{DOB}(j\omega)|}, \qquad \forall\omega \qquad (33)$$

where

$$\begin{aligned} T^n_{DOB}(s) &= \frac{P_n(s)Q(s)}{P_m(s) + [P_n(s)-P_m(s)]Q(s)} \\ &= \frac{L_n(s)}{1+L_n(s)} = G_{L_n}(s). \end{aligned} \qquad (34)$$

Proof. This theorem can be easily proved based on small gain theorem [13]. ■

It is noted from (33) that the robust stability condition is only dependent on the nominal closed-loop transfer function of the unity feedback system in the Fig. 4 and $|\Delta_M(j\omega)| < 1$ in low frequency range because $|G_{L_n}(j\omega)| \approx 1$ in that range. Hence $P_n(s)$ should be selected so that the difference between $P_n(s)$ and $P(s)$ is not too large in low frequency range, that is, $P_n(s)$ should satisfy $|[P(j\omega)-P_n(j\omega)]/P_n(j\omega)| < 1$ for robust stability. It is also noted that $|G_{L_n}(j\omega)|$ must be small at high frequencies, because uncertainty bound $|\Delta_M(j\omega)|$ is usually large in the high frequency range. If $K(s)$ is designed to stabilize $P_n(s)$, the above condition can be naturally satisfied. Therefore, $P_m(s)$ can be arbitrarily chosen as a proper function without RHP poles. This is also verified from Fig. 4. Of course, an external-loop controller should be designed considering $P_m(s)$ to avoid an inverse effect such as control input saturation.

The proposed DOB design in the RIC framework can be easily applied to general multivariable systems in a similar manner because the model following error can be defined in the RIC framework and the compensator $K(s)$ can be designed by general control theories based on a feedback error, and also Q-filter can be design independently on the sensitivity of the system.

4.3 Simulation

Let's take an example to achieve optimized mixed sensitivity and a specified transfer function of reference model $P_m(s)$ in the DOB design of Section 3. If $P_m(s)$ is given by $\frac{1}{J_m s^2}$ where J_m is 0.6 V/(m/s^2), then the multiplicative uncertainty and the disturbance defined based on reference model are obtained as follows:

$$\begin{aligned} \Delta^*_M(s) &= \frac{0.4s-0.1}{0.2s+0.1}, \\ d^* &= \left(\frac{0.4s-0.1}{0.2s+0.1}\right)u + \left(\frac{0.6s}{0.2s+0.1}\right)d_{ex}. \end{aligned} \qquad (35)$$

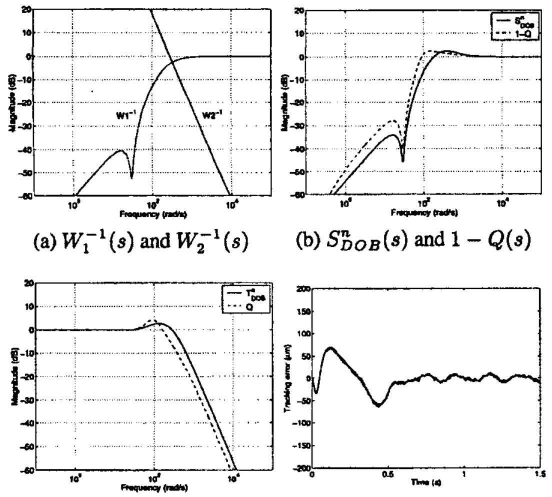

(a) $W_1^{-1}(s)$ and $W_2^{-1}(s)$ (b) $S_{DOB}^n(s)$ and $1 - Q(s)$

(c) $T_{DOB}^n(s)$ and $Q(s)$ (d) Tracking error

Figure 10: Designed sensitivity functions and tracking error

Thus, it can be known that the direct $Q(s)$ and $1 - Q(s)$ optimization is not proper to this problem since the mismatch becomes large. In this situation, the proposed sensitivity optimization method independent of $Q(s)$ should be used.

As one of the methods for mixed sensitivity optimization, let us consider $\mathcal{H}_\infty$ mixed sensitivity optimization because it is the most typical and popular method. Hence the optimal $K(s)$ is designed based on $\mathcal{H}_\infty$ mixed sensitivity method. In the mixed sensitivity problem formulation, nominal disturbance attenuation specifications and stability margin specifications are combined into a single infinity norm specification. Thus, the mixed $\mathcal{H}_\infty$ sensitivity problem is formulated as

$$\min_{K(s)} \left\| \begin{bmatrix} W_1(s)\, S_{DOB}^n(s) \\ W_2(s)\, T_{DOB}^n(s) \end{bmatrix} \right\|_\infty < 1 \tag{36}$$

where $S_{DOB}^n(s) = \frac{1}{1+L_n(s)}$ and $T_{DOB}^n(s) = \frac{L_n(s)}{1+L_n(s)}$. From the results of previous simulation, it was observed that the 30 rad/s sinusoid disturbance signal in Fig. 6 (a) is the main difficulty. Therefore, $K(s)$ should be optimized to further enhance the performance considering this frequency disturbance. In this example, the frequency domain specification is chosen as shown in Fig. 10 (a). Therefore the optimal RIC compensator can be obtained as follows:

$$K(s) = \frac{(1.5879 \times 10^9)s^3 + (1.3018 \times 10^{11})s^2}{s^4 + (3.5677 \times 10^4)s^3 + (2.2774 \times 10^7)s^2} \frac{+(3.2579 \times 10^{12})s + (1.4915 \times 10^{12})}{+(1.1147 \times 10^8)s + (2.0390 \times 10^{10})}. \tag{37}$$

The resulting $S_{DOB}^n(s)$ and $T_{DOB}^n(s)$ are shown in Fig. 10 (b) and (c). By substituting $K(s)$ into (30), the $1 - Q(s)$ and $Q(s)$ are obtained as shown in Fig. 10 (b) and (c). Note here that the $S_{DOB}^n(s)$ and $T_{DOB}^n(s)$ are not the same as $1 - Q(s)$ and $Q(s)$. If the controller in (19) is used as a feedback controller, then the tracking error is obtained as shown in Fig. 10 (d). In a similar manner, many kinds of feedback controllers can be used as mixed sensitivity optimization method for DOB in the RIC framework.

5 Conclusion

It was shown that there are inherent equivalences between RIC and DOB, and the proposed RIC structure can give general design framework for DOB algorithms by introducing the concept of reference model $P_m(s)$. Through this equivalent characteristics, design of DOB can be done systematically. The equivalent characteristics of these compensators and the validity of the proposed design method were verified by simulation. Mixed sensitivity optimization method for DOB design was also proposed through the parameterization in the RIC framework. Different from conventional methods, Q-filter was separately designed in the mixed sensitivity optimization. Thus, this guarantees the robustness and optimality of the DOB and also enables the design for unstable plants.

References

[1] K. Ohnishi, "A new servo method in mechatronics," *Trans. Japanese Society of Electrical Engineering*, vol. 107-D, pp. 83–86, 1987.

[2] T. Umeno, T. Kaneko, and Y. Hori, "Robust servosystem design with two degrees of freedom and its application to novel motion control of robot manipulators," *IEEE Trans. Industrial Electronics*, vol. 40, no. 5, pp. 473–485, 1993.

[3] K. Yamada, S. Komada, M. Ishida, and T. Hori, "Analysis and classical control design of servo system using high order disturbance observer," in *Proc. 1997 IEEE Int. Conf. on Industrial Electronics, Control, and Instrumentation*, pp. 4–9, 1997.

[4] B. K. Kim and W. K. Chung, "Performance predictable design of robust motion controllers for high-precision servo systems," in *Proc. 2001 American Control Conference*, pp. 2249–2254, 2001.

[5] B. K. Kim and W. K. Chung, "Unified analysis and design of robust disturbance attenuation algorithms using inherent structural equivalence," in *Proc. 2001 American Control Conference*, pp. 4046–4051, 2001.

[6] B. K. Kim, H.-T. Choi, W. K. Chung, and I. H. Suh, "Analysis and design of robust motion controllers in the unified framework," *ASME J. of Dyn. Syst., Meas. and Contr.*, vol. 124, 2002.

[7] B. K. Kim and W. K. Chung, "Performance tuning of sliding mode controllers : Structural analysis approach," in *Proc. 2001 American Control Conference*, pp. 1513–1518, 2001.

[8] B. K. Kim, H. T. Choi, W. K. Chung, I. H. Suh, H. S. Lee, and Y. H. Chang, "Robust time optimal controller design for HDD," *IEEE Trans. Magnetics*, vol. 35, no. 5, pp. 3598–3600, 1999.

[9] H. S. Lee and M. Tomizuka, "Robust motion controller design for high-accuracy positioning systems," *IEEE Trans. Industrial Electronics*, vol. 43, no. 1, pp. 48–55, 1996.

[10] M. Green and D. J. N. Limebeer, *Linear Robust Control*. Prentice-Hall, Inc., 1995.

[11] H.-T. Choi, B. K. Kim, I. H. Suh, and W. K. Chung, "Design of robust high-speed motion controller for a plant with actuator saturation," *ASME J. of Dyn. Syst., Meas. and Contr.*, vol. 122, no. 3, pp. 535–541, 2000.

[12] S. Park, B. K. Kim, and Y. Youm, "Single mode vibration suppression for a beam–mass–cart system using input preshaping with a robust internal–loop compensator," *J. of Sound and Vibration*, vol. 241, no. 4, pp. 693–716, 2001.

[13] J. C. Doyle, B. A. Francis, and A. R. Tannenbaum, *Feedback Control Theory*. Macmillan Publishing Co., 1992.